

# Phase-dependent optical effects in a four-level quantum system near a plasmonic nanostructure

Emmanuel Paspalakis\* and Sofia Evangelou

*Materials Science Department, School of Natural Sciences, University of Patras, Patras 265 04, Greece*

Vassilios Yannopoulos

*Department of Physics, National Technical University of Athens, Athens 157 80, Greece*

Andreas F. Terzis

*Department of Physics, School of Natural Sciences, University of Patras, Patras 265 04, Greece*

(Received 23 July 2013; published 21 November 2013)

We study the linear absorption and dispersion properties of a four-level double-V-type quantum system near a plasmonic nanostructure. The quantum system interacts with two orthogonal circularly polarized laser fields with the same frequency and different phases and electric field amplitudes. We find that the presence of the plasmonic nanostructure leads to strong modification of the absorption and dispersion spectra for one of the laser fields, in the presence of the other, and show that one can use the phase difference and the relative electric field amplitudes of the two laser fields for efficient control of the optical properties of the system. Effects such as complete optical transparency, zero absorption with nonzero dispersion, and gain without inversion are obtained.

DOI: [10.1103/PhysRevA.88.053832](https://doi.org/10.1103/PhysRevA.88.053832)

PACS number(s): 42.50.Gy, 42.50.Nn, 73.20.Mf, 78.67.Bf

## I. INTRODUCTION

Recent studies have revealed that several coherent optical phenomena can be strongly modified in quantum systems near plasmonic nanostructures. Examples of these phenomena include quantum interference effects in spontaneous emission [1–5], controlled population dynamics [6–11], optical transparency and slow light [12–15], and enhanced second harmonic generation and nonlinear optical switching [16,17], as well as gain without inversion [18,19]. In addition, phase-dependent effects in spontaneous emission lineshapes [20,21], unexpected population inversions [22,23], controlled absorption and dispersion [24–26], and slow light [26] have been studied in multilevel quantum systems that exhibit quantum interference in spontaneous emission.

In this work we study phase-dependent effects on the linear absorption and dispersion properties of a four-level double-V-type quantum system near a plasmonic nanostructure. In the quantum system under study one V-type transition is influenced by the interaction with surface plasmons, while the other V-type transition interacts with free-space vacuum. As a plasmonic nanostructure we consider a two-dimensional (2D) array of metal-coated dielectric nanospheres and calculate the relevant decay rates by a rigorous electromagnetic Green-tensor technique [1–3,14]. The quantum system interacts with two orthogonal circularly polarized laser fields with the same frequency and different phases and electric-field amplitudes, which couple the lowest state with the upper states in the free-space transitions. We use a density matrix methodology for the calculation of the linear susceptibility and show that the presence of the plasmonic nanostructure leads to strong modification of the absorption and dispersion spectra for one of the laser fields, in the presence of the other. In addition, we show that one can use the phase difference and the relative

electric-field amplitudes of the two laser fields for efficient control of the optical properties of the system. Effects such as complete optical transparency, zero absorption with nonzero dispersion, and gain without inversion are shown, and the conditions under which these phenomena occur are presented.

The article is organized as follows. In Sec. II we employ the density matrix equations for the interaction of the double-V-type system with the laser fields and the plasmonic nanostructure in order to calculate the linear susceptibility of the system. Then, in Sec. III we present results for the phase dependence of the absorption and dispersion spectra for different parameters of the system. Finally, in Sec. IV we summarize our findings.

## II. THEORETICAL MODEL AND CALCULATION OF THE LINEAR SUSCEPTIBILITY

The quantum system of interest is shown in Fig. 1. We consider a four-level system with two closely lying upper states,  $|2\rangle$  and  $|3\rangle$ , and two lower states,  $|0\rangle$  and  $|1\rangle$ . We call this system a double-V-type system, in order easily to identify two different three-level V-type transitions in the structure. The quantum system is located in vacuum at distance  $d$  from the surface of the plasmonic nanostructure. We take states  $|2\rangle$  and  $|3\rangle$  to characterize two Zeeman sublevels. Then the dipole moment operator is taken as  $\vec{\mu} = \mu'(|2\rangle\langle 0|\hat{\epsilon}_- + |3\rangle\langle 0|\hat{\epsilon}_+) + \mu(|2\rangle\langle 1|\hat{\epsilon}_- + |3\rangle\langle 1|\hat{\epsilon}_+) + \text{H.c.}$ , where  $\hat{\epsilon}_\pm = (\mathbf{e}_z \pm i\mathbf{e}_x)/\sqrt{2}$  describe the right-rotating ( $\hat{\epsilon}_+$ ) and left-rotating ( $\hat{\epsilon}_-$ ) unit vectors and  $\mu$  and  $\mu'$  are taken to be real.

The quantum system interacts with two circularly polarized continuous-wave electromagnetic (laser) fields, with total electric field

$$\vec{E}(t) = \hat{\epsilon}_+ E_a \cos(\omega_a t + \phi_a) + \hat{\epsilon}_- E_b \cos(\omega_b t + \phi_b), \quad (1)$$

where  $E_a$  ( $E_b$ ) is the electric-field amplitude,  $\omega_a$  ( $\omega_b$ ) is the angular frequency, and  $\phi_a$  ( $\phi_b$ ) is the phase of field  $a$  ( $b$ ). Laser

\*paspalak@upatras.gr

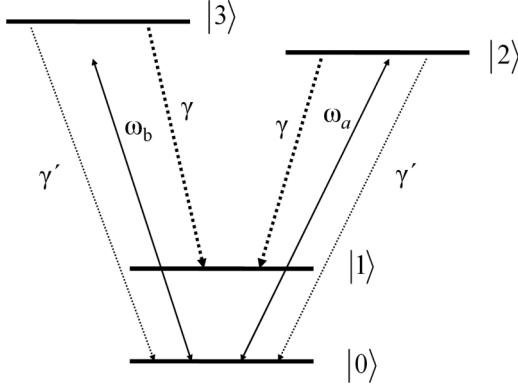


FIG. 1. The quantum system under study is a double-V-type system where two upper states,  $|2\rangle$  and  $|3\rangle$ , decay with spontaneous emission to the two lower states,  $|0\rangle$  and  $|1\rangle$ . The system also interacts with two circularly polarized weak probe laser fields with equal frequencies  $\omega_a = \omega_b$ . Laser field  $a$  couples state  $|0\rangle$  with state  $|2\rangle$  and laser field  $b$  couples state  $|0\rangle$  with state  $|3\rangle$ .

field  $a$  couples state  $|0\rangle$  with state  $|2\rangle$  and laser field  $b$  couples state  $|0\rangle$  with state  $|3\rangle$ . We assume that both fields have equal frequencies  $\omega_a = \omega_b = \omega$ . The Hamiltonian that describes the interaction of the electromagnetic field with the quantum system, in the dipole and rotating-wave approximations, is given by

$$H = \hbar \left( -\delta - \frac{\omega_{32}}{2} \right) |2\rangle \langle 2| + \hbar \left( -\delta + \frac{\omega_{32}}{2} \right) |3\rangle \langle 3| - \left( \frac{\hbar \Omega_a e^{i\phi_a}}{2} |0\rangle \langle 2| + \frac{\hbar \Omega_b e^{i\phi_b}}{2} |0\rangle \langle 3| + \text{H.c.} \right). \quad (2)$$

Here,  $\delta = \omega - \tilde{\omega}$  is the detuning from resonance with the average transition energies of states  $|2\rangle$  and  $|3\rangle$  from state  $|0\rangle$ , with  $\tilde{\omega} = (\omega_3 + \omega_2)/2 - \omega_0$ ,  $\omega_{32} = (\omega_3 - \omega_2)/2$ , and  $\Omega_a$  and  $\Omega_b$  are the Rabi frequencies for fields  $a$  and  $b$ , respectively, defined as  $\Omega_a = \mu' E_a / \hbar$  and  $\Omega_b = \mu' E_b / \hbar$ . Also,  $\hbar \omega_n$ , with  $n = 0 - 3$ , is the energy of state  $|n\rangle$ . We note that Eq. (2) describes only the interaction with the external laser fields. The quantum system also interacts with the vacuum and this process leads to spontaneous emission. For the form of the interaction Hamiltonian of the quantum system with the vacuum, see Eq. (28) of Ref. [27].

Both excited state  $|2\rangle$  and excited state  $|3\rangle$  decay spontaneously to state  $|0\rangle$  with decay rates  $2\gamma'_2$  and  $2\gamma'_3$ , respectively, and to state  $|1\rangle$  with decay rates  $2\gamma_2$  and  $2\gamma_3$ , respectively. We assume that transitions from  $|2\rangle$  and  $|3\rangle$  to  $|1\rangle$  lie within the surface-plasmon bands of the plasmonic nanostructure, whereas transitions from  $|2\rangle$  and  $|3\rangle$  to  $|0\rangle$  are spectrally distant from the surface-plasmon bands and are not influenced by the plasmonic nanostructure. Therefore, in transitions from  $|2\rangle$  and  $|3\rangle$  to  $|0\rangle$  the spontaneous decay occurs due to the interaction of the quantum system with free-space vacuum modes. In what follows, we refer to this decay as free-space spontaneous decay. We choose the energy difference of states  $|2\rangle$  and  $|3\rangle$  to be rather small, i.e.,  $\omega_{32}$  to be just a few  $\Gamma_0$ , where  $\Gamma_0$  is the decay rate of states  $|2\rangle$  and  $|3\rangle$  to state  $|1\rangle$  in the vacuum. The latter is taken to be the same for both states. We can therefore assume that  $\gamma_2 = \gamma_3 = \gamma$  and  $\gamma'_2 = \gamma'_3 = \gamma'$  [2].

Using the Hamiltonian of Eq. (2) we obtain the following equations for the density matrix elements of the system, assuming a Markovian response:

$$\dot{\rho}_{00}(t) = 2\gamma'[\rho_{22}(t) + \rho_{33}(t)] - i \frac{\Omega_a}{2} [\rho_{02}(t) e^{-i\phi_a} - \rho_{20}(t) e^{i\phi_a}] - i \frac{\Omega_b}{2} [\rho_{03}(t) e^{-i\phi_b} - \rho_{30}(t) e^{i\phi_b}], \quad (3)$$

$$\dot{\rho}_{22}(t) = -2(\gamma + \gamma')\rho_{22}(t) + i \frac{\Omega_a}{2} [\rho_{02}(t) e^{-i\phi_a} - \rho_{20}(t) e^{i\phi_a}] - \kappa[\rho_{23}(t) + \rho_{32}(t)], \quad (4)$$

$$\dot{\rho}_{33}(t) = -2(\gamma + \gamma')\rho_{33}(t) + i \frac{\Omega_b}{2} [\rho_{03}(t) e^{-i\phi_b} - \rho_{30}(t) e^{i\phi_b}] - \kappa[\rho_{23}(t) + \rho_{32}(t)], \quad (5)$$

$$\dot{\rho}_{20}(t) = \left( i\delta + i \frac{\omega_{32}}{2} - \gamma - \gamma' \right) \rho_{20}(t) + i \frac{\Omega_a}{2} e^{-i\phi_a} [\rho_{00}(t) - \rho_{22}(t)] - i \frac{\Omega_b}{2} e^{-i\phi_b} \rho_{23}(t) - \kappa \rho_{30}(t), \quad (6)$$

$$\dot{\rho}_{30}(t) = \left( i\delta - i \frac{\omega_{32}}{2} - \gamma - \gamma' \right) \rho_{30}(t) + i \frac{\Omega_b}{2} e^{-i\phi_b} [\rho_{00}(t) - \rho_{33}(t)] - i \frac{\Omega_a}{2} e^{-i\phi_a} \rho_{32}(t) - \kappa \rho_{20}(t), \quad (7)$$

$$\dot{\rho}_{23}(t) = (i\omega_{32} - 2\gamma - 2\gamma')\rho_{23}(t) + i \frac{\Omega_a}{2} e^{-i\phi_a} \rho_{03}(t) - i \frac{\Omega_b}{2} e^{i\phi_b} \rho_{20}(t) - \kappa[\rho_{22}(t) + \rho_{33}(t)], \quad (8)$$

with  $\rho_{00}(t) + \rho_{11}(t) + \rho_{22}(t) + \rho_{33}(t) = 1$  and  $\rho_{nm}(t) = \rho_{mn}^*(t)$ . Here,  $\kappa$  is the coupling coefficient between state  $|2\rangle$  and state  $|3\rangle$  due to spontaneous emission in a modified anisotropic vacuum [28] and it is responsible for the appearance of quantum interference [29].

The values of  $\gamma$  and  $\kappa$  are obtained by [30–33]

$$\gamma = \frac{\mu_0 \mu^2 \bar{\omega}^2}{\hbar} \hat{\epsilon}_- \cdot \text{Im} \mathbf{G}(\mathbf{r}, \mathbf{r}; \bar{\omega}) \cdot \hat{\epsilon}_+, \quad (9)$$

$$\kappa = \frac{\mu_0 \mu^2 \bar{\omega}^2}{\hbar} \hat{\epsilon}_+ \cdot \text{Im} \mathbf{G}(\mathbf{r}, \mathbf{r}; \bar{\omega}) \cdot \hat{\epsilon}_+. \quad (10)$$

Here,  $\mathbf{G}(\mathbf{r}, \mathbf{r}; \omega)$  is the dyadic electromagnetic Green's tensor, where  $\mathbf{r}$  refers to the position of the quantum emitter, and  $\mu_0$  is the permeability of vacuum. Also,  $\bar{\omega} = (\omega_3 + \omega_2)/2 - \omega_1$ . From Eqs. (9) and (10) we obtain the values of  $\gamma$  and  $\kappa$  as [30–33]

$$\gamma = \frac{\mu_0 \mu^2 \bar{\omega}^2}{2\hbar} \text{Im}[G_{\perp}(\mathbf{r}, \mathbf{r}; \bar{\omega}) + G_{\parallel}(\mathbf{r}, \mathbf{r}; \bar{\omega})] = \frac{1}{2}(\Gamma_{\perp} + \Gamma_{\parallel}), \quad (11)$$

$$\kappa = \frac{\mu_0 \mu^2 \bar{\omega}^2}{2\hbar} \text{Im}[G_{\perp}(\mathbf{r}, \mathbf{r}; \bar{\omega}) - G_{\parallel}(\mathbf{r}, \mathbf{r}; \bar{\omega})] = \frac{1}{2}(\Gamma_{\perp} - \Gamma_{\parallel}). \quad (12)$$

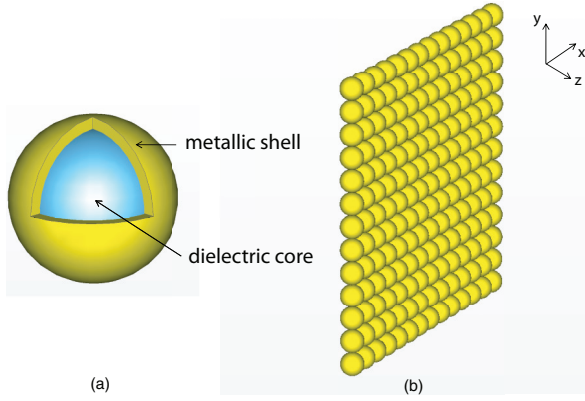


FIG. 2. (Color online) (a) A metal-coated dielectric nanosphere and (b) a 2D array of such spheres used in this work.

Here,  $G_{\perp}(\mathbf{r}, \mathbf{r}; \bar{\omega}) = G_{zz}(\mathbf{r}, \mathbf{r}; \bar{\omega})$  and  $G_{\parallel}(\mathbf{r}, \mathbf{r}; \bar{\omega}) = G_{xx}(\mathbf{r}, \mathbf{r}; \bar{\omega})$  denote components of the electromagnetic Green's tensor, where the symbol  $\perp$  ( $\parallel$ ) refers to a dipole oriented normal—along the  $z$  axis (parallel—along the  $x$  axis) to the surface of the nanostructure. Finally, we define the spontaneous emission rates normal and parallel to the surface as  $\Gamma_{\perp, \parallel} = \mu_0 \mu^2 \bar{\omega}^2 \text{Im}[G_{\perp, \parallel}(\mathbf{r}, \mathbf{r}; \bar{\omega})]/\hbar$ . The degree of quantum interference is defined as  $p = (\Gamma_{\perp} - \Gamma_{\parallel})/(\Gamma_{\perp} + \Gamma_{\parallel})$ . For  $p = 1$  we have maximum quantum interference in spontaneous emission [29]. This can be achieved by placing the emitter close to a structure that completely quenches  $\Gamma_{\parallel}$ . We stress that when the emitter is placed in vacuum,  $\Gamma_{\perp} = \Gamma_{\parallel}$  and  $\kappa = 0$ , so no quantum interference occurs in the system.

The plasmonic nanostructure considered in this study is a 2D array of touching metal-coated silica nanospheres [see Figs. 2(a) and 2(b)]. Periodic arrays of metallic nanoshells can be fabricated via self-assembly [34,35], nanopatterning and nanolithographic [36,37] techniques. The dielectric function of the shell is provided by a Drude-type electric permittivity given by

$$\epsilon(\omega) = 1 - \frac{\omega_p^2}{\omega(\omega + i/\tau)}, \quad (13)$$

where  $\omega_p$  is the bulk plasma frequency and  $\tau$  the relaxation time of the conduction-band electrons of the metal. A typical value of the plasma frequency for gold is  $\hbar\omega_p = 8.99$  eV. This also determines the length scale of the system as  $c/\omega_p \approx 22$  nm. The dielectric constant of  $\text{SiO}_2$  is taken to be  $\epsilon = 2.1$ . In the calculations we have taken  $\tau^{-1} = 0.05\omega_p$ . The lattice constant of the square lattice is  $a = 2c/\omega_p$  and the sphere radius  $S = c/\omega_p$  with core radius  $S_c = 0.7c/\omega_p$ .

The electromagnetic Green's tensor providing the corresponding spontaneous emission rates  $\Gamma_{\perp}$  and  $\Gamma_{\parallel}$  is given by [1,38,39]

$$G_{ii'}^{EE}(\mathbf{r}, \mathbf{r}'; \omega) = g_{ii'}^{EE}(\mathbf{r}, \mathbf{r}'; \omega) - \frac{i}{8\pi^2} \int \int_{\text{SBZ}} d^2\mathbf{k}_{\parallel} \sum_{\mathbf{g}} \frac{1}{c^2 \mathbf{K}_{\mathbf{g};z}^{\pm}} \times v_{\mathbf{g}\mathbf{k}_{\parallel};i}(\mathbf{r}) \exp(-i\mathbf{K}_{\mathbf{g}}^+ \cdot \mathbf{r}) \hat{\mathbf{e}}_i(\mathbf{K}_{\mathbf{g}}^+), \quad (14)$$

with

$$v_{\mathbf{g}\mathbf{k}_{\parallel};i}(\mathbf{r}) = \sum_{\mathbf{g}'} R_{\mathbf{g}'\mathbf{g}}(\omega, \mathbf{k}_{\parallel}) \exp(-i\mathbf{K}_{\mathbf{g}'}^- \cdot \mathbf{r}) \hat{\mathbf{e}}_i(\mathbf{K}_{\mathbf{g}'}^-) \quad (15)$$

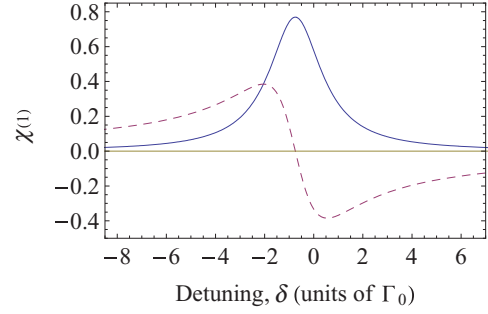


FIG. 3. (Color online) Absorption spectrum [ $\text{Im}(\chi^{(1)})$ ; solid curve] and dispersion spectrum [ $\text{Re}(\chi^{(1)})$ ; dashed curve] of the quantum system in units of  $N\mu^2/(\hbar\epsilon_0\Gamma_0)$ , as given by Eq. (20), in the absence of the plasmonic nanostructure. We take  $\omega_{32} = 1.5\Gamma_0$  and  $\gamma' = 0.3\Gamma_0$ .

and

$$\mathbf{K}_{\mathbf{g}}^{\pm} = \{\mathbf{k}_{\parallel} + \mathbf{g}, \pm [q^2 - (\mathbf{k}_{\parallel} + \mathbf{g})^2]^{1/2}\}. \quad (16)$$

The vectors  $\mathbf{g}$  denote the reciprocal-lattice vectors corresponding to the 2D periodic lattice of the plane of scatterers, and  $\mathbf{k}_{\parallel}$  is the reduced wave vector which lies within the surface Brillouin zone associated with the reciprocal lattice [40]. When  $q^2 = \omega^2/c^2 < (\mathbf{k}_{\parallel} + \mathbf{g})^2$ ,  $\mathbf{K}_{\mathbf{g}}^{\pm}$  defines an evanescent wave. The term  $g_{ii'}^{EE}(\mathbf{r}, \mathbf{r}'; \omega)$  in Eq. (14) is the free-space Green's tensor, and  $\hat{\mathbf{e}}_i(\mathbf{K}_{\mathbf{g}}^{\pm})$  the polar unit vector normal to  $\mathbf{K}_{\mathbf{g}}^{\pm}$ .  $R_{\mathbf{g}'\mathbf{g}}(\omega, \mathbf{k}_{\parallel})$  is the reflection matrix, which provides the sum (over  $\mathbf{g}$ 's) of reflected beams generated by the incidence of a plane wave from the left of the plane of scatterers [40]. Also, in Eq. (14), the terms corresponding to  $s$ -polarized waves [those containing components with the azimuthal unit vector  $\hat{\mathbf{e}}_i(\mathbf{K}_{\mathbf{g}}^{\pm})$  normal to  $\mathbf{K}_{\mathbf{g}}^{\pm}$ ] make a small contribution to the decay rates and have, therefore, been neglected.

We take  $\bar{\omega} = 0.632\omega_p$  and the distance between the quantum system and the surface of the plasmonic nanostructure,  $d$ , to vary from  $0.5c/\omega_p$  to  $c/\omega_p$ . For the results of  $\Gamma_{\perp}$  and  $\Gamma_{\parallel}$  that are used in the present work, we refer to Fig. 3 in Ref. [14]. We find that  $\Gamma_{\parallel}$  exhibits significant suppression and its actual value becomes significantly lower than the free-space decay rate. In addition, the value of  $\Gamma_{\perp}$  decreases with increasing distance between the quantum system and the plasmonic nanostructure. For distances close to the plasmonic nanostructure,  $\Gamma_{\perp}$  becomes much larger than the free-space decay rate. The value of  $\Gamma_{\perp}$  is larger than the free-space decay rate for distances up to  $0.6c/\omega_p$ , while for distances between  $0.65c/\omega_p$  and  $c/\omega_p$  the value of  $\Gamma_{\perp}$  becomes lower than the free-space decay rate.

The absorption and dispersion response for a weak laser field  $a$  is determined by the linear electric susceptibility, which is given by [26,41]

$$\chi^{(1)}(\omega) = \frac{2N\mu'}{\epsilon_0 E_a e^{-i\phi_a}} \rho_{20}^{(1)} = \frac{2N\mu'^2 e^{i\phi_a}}{\epsilon_0 \hbar} \frac{\rho_{20}^{(1)}}{\Omega_a}, \quad (17)$$

where  $\rho_{20}^{(1)}$  is calculated in the steady state and in first order in terms of  $E_a$  (or  $\Omega_a$ ),  $\epsilon_0$  is the vacuum permittivity, and  $N$  is the density of the quantum systems.

Using perturbation theory and assuming that both field  $a$  and field  $b$  are weak fields, we obtain from Eqs. (3)–(8), after

some algebra,

$$\rho_{20}^{(1)} = \frac{i \frac{\Omega_a}{2} e^{-i\phi_a} (-i\delta + i \frac{\omega_{32}}{2} + \gamma + \gamma') - i\kappa \frac{\Omega_b}{2} e^{-i\phi_b}}{(-i\delta + i \frac{\omega_{32}}{2} + \gamma + \gamma')(-i\delta - i \frac{\omega_{32}}{2} + \gamma + \gamma') - \kappa^2}. \quad (18)$$

We substitute  $\rho_{20}^{(1)}$  from Eq. (18) into Eq. (17) and obtain

$$\chi^{(1)}(\delta) = \frac{N\mu^2}{\varepsilon_0 \hbar} \frac{\delta - \frac{\omega_{32}}{2} + i\gamma + i\gamma' - i\kappa \frac{E_b}{E_a} e^{i\phi}}{(-i\delta + i \frac{\omega_{32}}{2} + \gamma + \gamma')(-i\delta - i \frac{\omega_{32}}{2} + \gamma + \gamma') - \kappa^2}, \quad (19)$$

where  $\phi = \phi_a - \phi_b$  is the phase difference between the two applied fields.

### III. PHASE-DEPENDENT EFFECTS IN THE ABSORPTION AND DISPERSION SPECTRA

In Fig. 3 we present the real (determines dispersion) and imaginary (determines absorption) parts of  $\chi^{(1)}$  as a function of the detuning  $\delta$  with the quantum system in vacuum, i.e., without the plasmonic nanostructure. In this case,

$$\chi^{(1)}(\delta) = \frac{N\mu^2}{\varepsilon_0 \hbar} \frac{\delta - \frac{\omega_{32}}{2} + i\Gamma_0 + i\gamma'}{(-i\delta + \Gamma_0 + \gamma')^2 + \frac{\omega_{32}^2}{4}}. \quad (20)$$

There, typical absorption and dispersion spectra [41] are obtained, which are centered at  $\delta = -\omega_{32}/2$ . Also, no phase dependence is shown in this case.

The absorption and dispersion properties are very different when the quantum system is near the plasmonic

nanostructure. In order to obtain compact forms in the following analysis we define  $A = \frac{N\mu^2}{\varepsilon_0 \hbar}$ ,  $\tilde{\alpha} = \frac{\omega_{32}}{2}$ ,  $\tilde{\gamma} = \gamma + \gamma'$ ,  $x = \frac{E_b}{E_a}$ ,  $\alpha = \alpha(\phi, x) = \kappa x \sin \phi - \tilde{\alpha}$ ,  $\beta = \beta(\phi, x) = \tilde{\gamma} - \kappa x \cos \phi$ ,  $\varepsilon = \tilde{\alpha}^2 + \tilde{\gamma}^2 - \kappa^2 = \tilde{\alpha}^2 + (\Gamma_{\parallel} + \gamma')(\Gamma_{\perp} + \gamma')$  ( $>0$ ), and  $\zeta = -2\tilde{\gamma}$  ( $<0$ ). Then the real and imaginary parts of the susceptibility of Eq. (19) read as

$$\text{Re}[\chi^{(1)}(\delta)] = A \frac{(\alpha + \delta)(\varepsilon - \delta^2) + \beta\zeta\delta}{(\varepsilon - \delta^2)^2 + \zeta^2\delta^2} \quad (21)$$

and

$$\text{Im}[\chi^{(1)}(\delta)] = A \frac{\beta(\varepsilon - \delta^2) - \zeta\delta(\alpha + \delta)}{(\varepsilon - \delta^2)^2 + \zeta^2\delta^2}. \quad (22)$$

We first present the conditions corresponding to zero absorption ( $\text{Im}[\chi^{(1)}(\delta)] = 0$ ) but nonzero dispersion ( $\text{Re}[\chi^{(1)}(\delta)] \neq 0$ ), which leads to enhancement of the index of refraction without absorption [42,43]. We find that this occurs at detunings

$$\delta_{\pm} = \frac{\tilde{\gamma}(\tilde{\alpha} - \kappa x \sin \phi) \pm \sqrt{\tilde{\gamma}^2(\tilde{\alpha} - \kappa x \sin \phi)^2 + \varepsilon(\kappa^2 x^2 \cos^2 \phi - \tilde{\gamma}^2)}}{\tilde{\gamma} + \kappa x \cos \phi}. \quad (23)$$

This is accomplished if the quantity in the square root is positive or zero, leading to

$$\tilde{\gamma}^2(\tilde{\alpha} - \kappa x \sin \phi)^2 \geq \varepsilon(\tilde{\gamma}^2 - \kappa^2 x^2 \cos^2 \phi). \quad (24)$$

When  $\delta = 0$  or  $\omega = \tilde{\omega}$  (at this particular frequency the system exhibits strong absorption suppression when it interacts with a linearly polarized laser field [14]), Eq. (23) leads to  $x^2 \kappa^2 \cos^2 \phi = \tilde{\gamma}^2$  or, for positive  $\cos \phi$ ,

$$\frac{E_b}{E_a} = \frac{\Gamma_{\perp} + \Gamma_{\parallel} + 2\gamma'}{(\Gamma_{\perp} - \Gamma_{\parallel}) \cos \phi}, \quad (25)$$

provided that  $\Gamma_{\perp} \neq \Gamma_{\parallel}$ . In this case,

$$\begin{aligned} \text{Re}[\chi^{(1)}(\delta = 0)] &= A \frac{\alpha}{\varepsilon} \\ &= \frac{N\mu^2}{2\varepsilon_0 \hbar} \frac{-\omega_{32} + (\Gamma_{\perp} + \Gamma_{\parallel} + 2\gamma') \tan \phi}{\frac{\omega_{32}^2}{4} + (\Gamma_{\parallel} + \gamma')(\Gamma_{\perp} + \gamma')}. \end{aligned} \quad (26)$$

Next, we present the conditions for exact optical transparency [ $\chi^{(1)}(\delta) = 0$ ]. From Eqs. (21) and (22) we obtain that

this occurs when  $\beta = 0$  and  $\delta = -\alpha$  or

$$\frac{E_b}{E_a} \cos \phi = \frac{\Gamma_{\perp} + \Gamma_{\parallel} + 2\gamma'}{\Gamma_{\perp} - \Gamma_{\parallel}} \quad (27)$$

and

$$\delta = \frac{\omega_{32}}{2} - \frac{\Gamma_{\perp} - \Gamma_{\parallel}}{2} \frac{E_b}{E_a} \sin \phi. \quad (28)$$

This means that exact optical transparency is possible for laser  $a$  in this system as long as  $\Gamma_{\perp} \neq \Gamma_{\parallel}$ , which is a typical case next to the plasmonic nanostructure [1]. In addition, the optical transparency here is exact and not approximate and can occur irrespective of the value of the free-space decay rate  $\gamma'$ , in contrast to the results found in Ref. [14], where the system interacts with a single linearly polarized laser field.

Furthermore, for  $\phi$  satisfying Eq. (27), Eq. (28) provides complete optical transparency at

$$\delta = \frac{\omega_{32}}{2} - \frac{1}{2} \sqrt{(\Gamma_{\perp} - \Gamma_{\parallel})^2 \frac{E_b^2}{E_a^2} - (\Gamma_{\perp} + \Gamma_{\parallel} + 2\gamma')^2}. \quad (29)$$

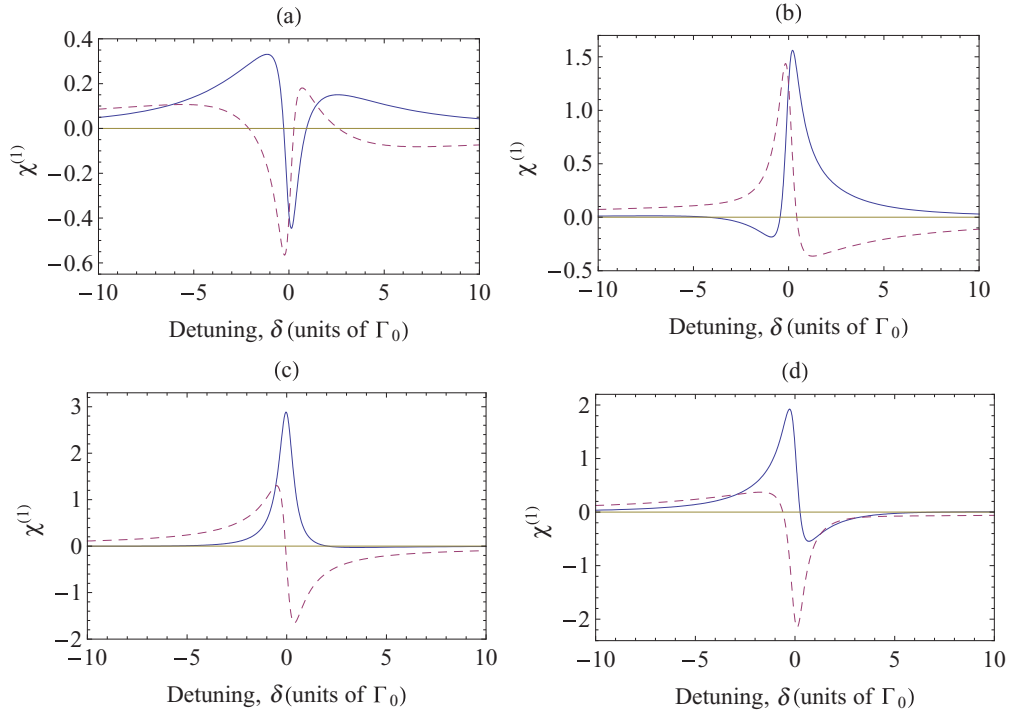


FIG. 4. (Color online) Absorption spectrum [ $\text{Im}(\chi^{(1)})$ ; solid curve] and dispersion spectrum [ $\text{Re}(\chi^{(1)})$ ; dashed curve] of the quantum system in units of  $N\mu'^2/(\hbar\epsilon_0\Gamma_0)$ , as given by Eq. (19), in the presence of the plasmonic nanostructure. We take  $\omega_{32} = 1.5\Gamma_0$ ,  $\gamma' = 0.3\Gamma_0$ ,  $E_b/E_a = 1.5$ ,  $\bar{\omega} = 0.632\omega_p$ , and  $d = 0.4c/\omega_p$ , leading to  $\Gamma_{\perp} = 4.132\Gamma_0$  and  $\Gamma_{\parallel} = 0.0031\Gamma_0$ . (a)  $\phi = 0$ , (b)  $\phi = \pi/2$ , (c)  $\phi = \pi$ , and (d)  $\phi = 3\pi/2$ .

We note that if the quantity in the square root is positive or 0 (which, in compact form, is written  $\kappa^2 x^2 \geq \tilde{\gamma}^2$ ), then complete optical transparency can always be obtained in the system.

When  $\delta = 0$ , we obtain that exact optical transparency is obtained for

$$\tan \phi = \frac{\omega_{32}}{\Gamma_{\perp} + \Gamma_{\parallel} + 2\gamma'} \quad (30)$$

and

$$\frac{E_b}{E_a} = \frac{\sqrt{\omega_{32}^2 + (\Gamma_{\perp} + \Gamma_{\parallel} + 2\gamma')^2}}{\Gamma_{\perp} - \Gamma_{\parallel}}. \quad (31)$$

If  $\omega_{32} = 0$ , then  $\phi = n\pi$  with  $n = 0, 1, 2, \dots$ , and Eq. (31) reduces to

$$\frac{E_b}{E_a} = \frac{\Gamma_{\perp} + \Gamma_{\parallel} + 2\gamma'}{\Gamma_{\perp} - \Gamma_{\parallel}}, \quad (32)$$

which, for  $\gamma' = 0$ , provided that  $\Gamma_{\perp} \gg \Gamma_{\parallel}$  (typical case next to the plasmonic nanostructure under study [1–3,14]), gives approximately  $E_a \approx E_b$ .

Furthermore, we can obtain gain [ $\text{Im}[\chi^{(1)}(\bar{\omega})] < 0$ ] in the system, which is without inversion, as the vast majority of population remains in state  $|0\rangle$ . The condition for gain without inversion is also given by Eq. (24). Then we can obtain gain without inversion between the values of  $\delta_-$  and  $\delta_+$  for  $\kappa x \cos \phi + \tilde{\gamma} > 0$  or

$$(\Gamma_{\perp} - \Gamma_{\parallel}) \frac{E_b}{E_a} \cos \phi + \Gamma_{\perp} + \Gamma_{\parallel} + 2\gamma' > 0, \quad (33)$$

which, for  $\cos \phi \geq 0$ , is always satisfied next to the plasmonic nanostructure. If, however,  $\kappa x \cos \phi + \tilde{\gamma} < 0$ , then we obtain gain outside the region  $[\delta_-, \delta_+]$ .

In Fig. 4 we present examples of the absorption and dispersion spectra for different phases  $\phi$  and for  $\frac{E_b}{E_a} = 1.5$  when the quantum system is placed at distance  $d = 0.4c/\omega_p$  from the surface of the plasmonic nanostructure. We see that the shape of the absorption and dispersion spectra is strongly influenced by the change of  $\phi$ . In addition, in all cases, zero absorption with nonzero dispersion and gain without inversion are obtained. The detuning values for zero absorption, which also determine the region of gain without inversion, change with  $\phi$  too, due to the dependence of  $\delta_{\pm}$  on phase  $\phi$  [see Eq. (23)].

Next, in Fig. 5 we present the absorption and dispersion spectra for the same parameters used in Fig. 4 but for a different distance of the quantum system from the plasmonic nanostructure,  $d = 0.7c/\omega_p$ . As the change in  $d$  leads to a change in the values of  $\Gamma_{\perp}$  and  $\Gamma_{\parallel}$ , the shape of the absorption and dispersion spectra in this case is rather different from that in Fig. 4. In addition, here we observe zero absorption with nonzero dispersion and gain without inversion [Figs. 5(a), 5(c), and 5(d)], as well as a case where only absorption appears [Fig. 5(b)].

Finally, in Fig. 6 we present two cases where complete optical transparency is obtained, namely, in Fig. 6(a) ( $d = 0.4c/\omega_p$ ) and in Fig. 6(b) ( $d = 0.7c/\omega_p$ ). In both cases the phase  $\phi$  is taken so as to satisfy Eq. (27). The shapes of the absorption and dispersion spectra are different in the two cases due to the difference in  $\Gamma_{\perp}$ ,  $\Gamma_{\parallel}$ , and  $\frac{E_b}{E_a}$ . However, complete optical transparency is obtained at a detuning given by Eq. (28)

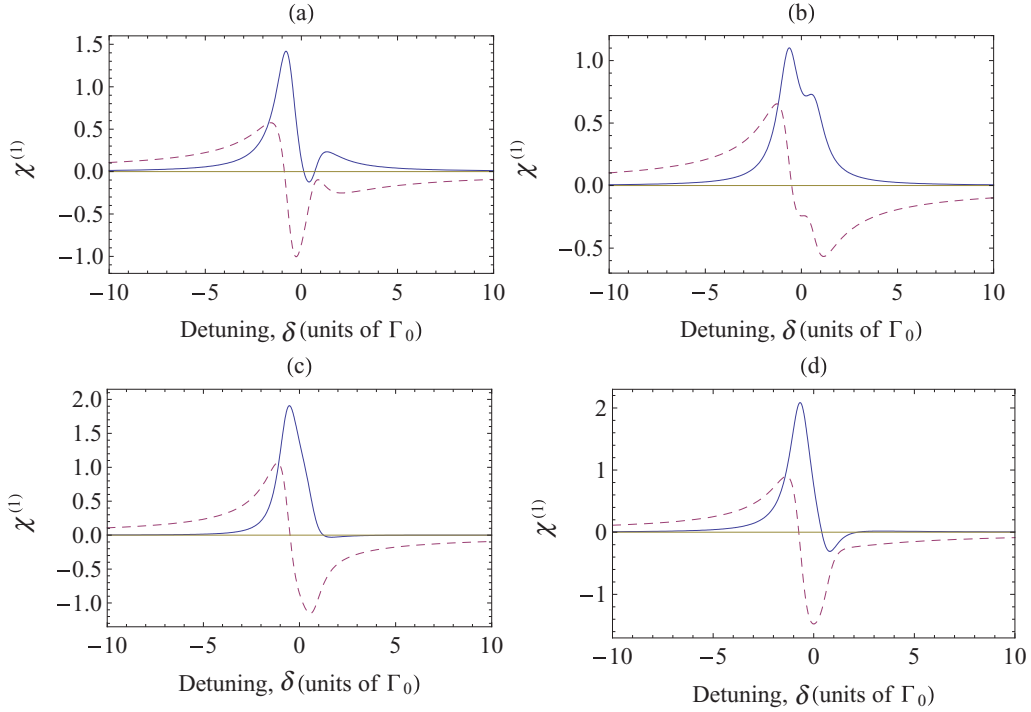


FIG. 5. (Color online) The same as Fig. 4, but with  $d = 0.7c/\omega_p$ , leading to  $\Gamma_{\perp} = 0.722\Gamma_0$  and  $\Gamma_{\parallel} = 0.0039\Gamma_0$ .

or (29). Besides complete optical transparency, zero absorption with nonzero dispersion at different frequencies as well as gain without inversion is also found. In addition, the dispersion

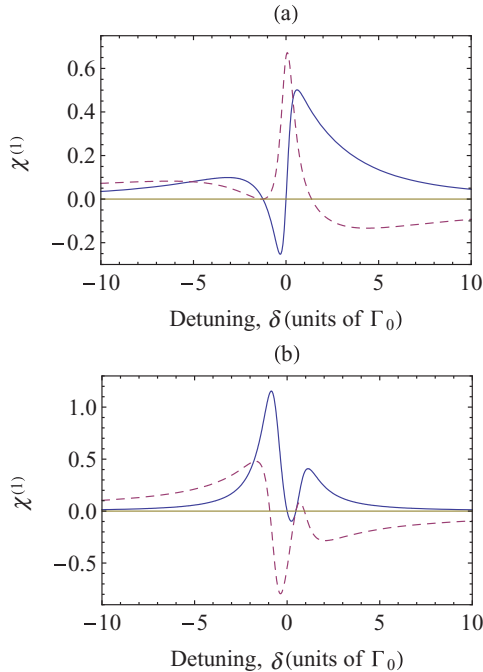


FIG. 6. (Color online) Absorption spectrum [ $\text{Im}(\chi^{(1)})$ ; solid curve] and dispersion spectrum [ $\text{Re}(\chi^{(1)})$ ; dashed curve] of the quantum system in units of  $N\mu^2/(\hbar\epsilon_0\Gamma_0)$ , as given by Eq. (19), in the presence of the plasmonic nanostructure. We take  $\omega_{32} = 1.5\Gamma_0$ ,  $\gamma' = 0.3\Gamma_0$ , and  $\tilde{\omega} = 0.632\omega_p$ . (a)  $d = 0.4c/\omega_p$  and  $E_b/E_a = 1.5$ . (b)  $d = 0.7c/\omega_p$  and  $E_b/E_a = 2$ . In both cases the phase  $\phi$  is chosen to satisfy Eq. (27).

curve near the transparency window behaves very differently in the two cases, implying that very different values of the group velocity are obtained.

Before closing this section we outline some possibilities for experimental realization of the double-V-type quantum system that we study here. As the transitions from  $|2\rangle$  to  $|1\rangle$  (or  $|0\rangle$ ) and from  $|3\rangle$  to  $|1\rangle$  (or  $|0\rangle$ ) have orthogonal dipole matrix elements, the quantum system can be realized in several atomic systems, having, for example, two  $J = 0$  states for the lower states,  $|0\rangle$  and  $|1\rangle$ , and  $M = \pm 1$  sublevels of a  $J = 1$  state for excited states  $|2\rangle$  and  $|3\rangle$ . The energy difference  $\hbar\omega_{32}$  can be changed by a static magnetic field. In addition, the quantum system may be realized in hyperfine sublevels of  $D$  lines in alkali-metal atoms like  $^{85}\text{Rb}$  and  $^{87}\text{Rb}$  [4,9,15] or in dual CdSe/ZnS/CdSe quantum dots [15].

Furthermore, the results presented above can also be realized in a regular (single) V-type system as well, where the optical transitions are influenced by the presence of the surface plasmons and the laser fields couple in these transitions [8,44]. In that case, however, the electric-field amplitudes may also be modified by the presence of the plasmonic nanostructure [4,15], and this should be properly taken into account by changing the initial values of the electric-field amplitudes. This quantum system may be realized in various atoms, using the prescription outlined above, as well as in semiconductor quantum dots, where state  $|0\rangle$  is the ground (no-exciton) state and the upper states are the left and right circularly polarized single-exciton states.

#### IV. SUMMARY

In this work we have studied the linear absorption and dispersion properties of a four-level double-V-type quantum system near a plasmonic nanostructure. In the quantum

system under study one V-type transition is influenced by the interaction with surface plasmons, while the other V-type transition interacts with free-space vacuum. As a plasmonic nanostructure we have considered a 2D array of metal-coated dielectric nanospheres, in which case we have calculated the relevant decay rates by a rigorous electromagnetic Green-tensor technique [1–3,14]. The quantum system interacts with two orthogonal circularly polarized laser fields with the same frequency and different phases and electric-field amplitudes, which couple the lowest state with the upper states in the free-space transitions. Using a density matrix methodology for the calculation of the linear susceptibility, we have shown that the presence of the plasmonic nanostructure leads to strong modification of the absorption and dispersion spectra of one of the laser fields, in the presence of the other. In addition, we have shown that the phase difference and the relative electric-field amplitudes of the two laser fields can be used for efficient control of the optical properties of the system. Effects such as complete optical transparency, zero absorption with nonzero dispersion, and gain without inversion have been identified, along with the conditions under which these phenomena occur.

We note in closing that from the above analysis we have found that the effects presented here are not limited to the specific plasmonic nanostructure studied in this work (2D array of metal-coated dielectric nanospheres) but can also occur in other plasmonic nanostructures, such as, for example, a metallic slab or a metallic nanosphere, where quantum interference effects in spontaneous emission can occur [1].

Furthermore, our analysis has revealed that the studied effects can also occur for large values of the free-space spontaneous emission rate with proper adjustment of the parameters of the phase difference and the relative electric-field amplitudes of the two laser fields. This is in contrast to the quantum coherence phenomena obtained when a single linearly polarized field interacts with the system [14]. Finally, in the present study we have assumed that the quantum system and the plasmonic nanostructure are in vacuum. The phenomena reported above are manifested even when the quantum system and the plasmonic nanostructure are embedded in a host matrix, as long as  $\Gamma_{\parallel}$  is different from  $\Gamma_{\perp}$ . In that case the electric-field amplitudes or the Rabi frequencies should be modified by the effective dielectric constant by taking into account the local field effect due to the dielectric mismatch [45]. Correspondingly, the values of  $\Gamma_{\parallel}$  and  $\Gamma_{\perp}$  will change. If the host matrix is a polymer with a low index of refraction (values from 1.3 to 1.4), then only weak quantitative changes will be observed.

#### ACKNOWLEDGMENTS

This research was cofinanced by the European Union (European Social Fund) and Greek national funds through the Operational Program “Education and Lifelong Learning” of the National Strategic Reference Framework–Research Funding Program Heracleitus II, Investing in Knowledge Society, through the European Social Fund.

- 
- [1] V. Yannopapas, E. Paspalakis, and N. V. Vitanov, *Phys. Rev. Lett.* **103**, 063602 (2009).
- [2] S. Evangelou, V. Yannopapas, and E. Paspalakis, *Phys. Rev. A* **83**, 023819 (2011).
- [3] S. Evangelou, V. Yannopapas, and E. Paspalakis, *Phys. Rev. A* **83**, 055805 (2011).
- [4] Y. Gu, L. Wang, P. Ren, J.-X. Zhang, T.-C. Zhang, O. J. F. Martin, and Q.-H. Gong, *Nano Lett.* **12**, 2488 (2012).
- [5] Y. Gu, L. Wang, P. Ren, J.-X. Zhang, T.-C. Zhang, J.-P. Xu, S.-Y. Zhu, and Q.-H. Gong, *Plasmonics* **7**, 33 (2012).
- [6] M.-T. Cheng, S.-D. Liu, H.-J. Zhou, Z.-H. Hao, and Q.-Q. Wang, *Opt. Lett.* **32**, 2125 (2007).
- [7] S. M. Sadeghi, *Nanotechnology* **20**, 225401 (2009); *Phys. Rev. B* **79**, 233309 (2009).
- [8] M. A. Antón, F. Carreño, S. Melle, O. G. Calderón, E. Cabrera-Granado, J. Cox, and M. R. Singh, *Phys. Rev. B* **86**, 155305 (2012).
- [9] M. Sukharev and S. A. Malinovskaya, *Phys. Rev. A* **86**, 043406 (2012).
- [10] M. A. Antón, F. Carreño, S. Melle, O. G. Calderón, E. Cabrera-Granado, and M. R. Singh, *Phys. Rev. B* **87**, 195303 (2013).
- [11] E. Paspalakis, S. Evangelou, and A. F. Terzis, *Phys. Rev. B* **87**, 235302 (2013).
- [12] Z. Lu and K.-D. Zhu, *J. Phys. B* **42**, 015502 (2009).
- [13] A. Hatef and M. R. Singh, *Phys. Rev. A* **81**, 063816 (2010).
- [14] S. Evangelou, V. Yannopapas, and E. Paspalakis, *Phys. Rev. A* **86**, 053811 (2012).
- [15] L. Wang, Y. Gu, H. Chen, J.-Y. Zhang, Y. Cui, B. D. Gerardot, and Q. Gong, *Sci. Rep.* **3**, 2879 (2013).
- [16] M. R. Singh, *Nanotechnology* **24**, 125701 (2013).
- [17] J. D. Cox, M. R. Singh, C. von Bilderling, and A. V. Bragas, *Adv. Opt. Mater.* **1**, 460 (2013).
- [18] S. M. Sadeghi, *Nanotechnology* **21**, 455401 (2010); *Phys. Rev. A* **88**, 013831 (2013).
- [19] S. G. Kosionis, A. F. Terzis, S. M. Sadeghi, and E. Paspalakis, *J. Phys.: Condens. Matter* **25**, 045304 (2013).
- [20] E. Paspalakis and P. L. Knight, *Phys. Rev. Lett.* **81**, 293 (1998).
- [21] M. Macovei, J. Evers, and C. H. Keitel, *Phys. Rev. Lett.* **91**, 233601 (2003).
- [22] S.-Q. Gong, E. Paspalakis, and P. L. Knight, *J. Mod. Opt.* **45**, 2433 (1998).
- [23] S.-Q. Gong, Y. Li, S.-D. Du, and Z.-Z. Xu, *Phys. Lett. A* **259**, 43 (1999).
- [24] J.-H. Wu and J.-Y. Gao, *Phys. Rev. A* **65**, 063807 (2002).
- [25] W.-H. Xu, J.-H. Wu, and J.-Y. Gao, *Phys. Rev. A* **66**, 063812 (2002).
- [26] D. Bortman-Arbiv, A. D. Wilson-Gordon, and H. Friedmann, *Phys. Rev. A* **63**, 043818 (2001).
- [27] H. Lee, P. Polynkin, M. O. Scully, and S.-Y. Zhu, *Phys. Rev. A* **55**, 4454 (1997).
- [28] G. S. Agarwal, *Phys. Rev. Lett.* **84**, 5500 (2000).
- [29] M. Kiffner, M. Macovei, J. Evers, and C. H. Keitel, in *Progress in Optics*, edited by E. Wolf, Vol. 55 (Elsevier, Amsterdam, 2010), p. 85.

- [30] G. X. Li, F.-L. Li, and S.-Y. Zhu, *Phys. Rev. A* **64**, 013819 (2001).
- [31] Y.-P. Yang, J.-P. Xu, H. Chen, and S.-Y. Zhu, *Phys. Rev. Lett.* **100**, 043601 (2008).
- [32] G.-X. Li, J. Evers, and C. H. Keitel, *Phys. Rev. B* **80**, 045102 (2009).
- [33] J.-P. Xu and Y.-P. Yang, *Phys. Rev. A* **81**, 013816 (2010).
- [34] H. Wang, J. Kundu, and N. J. Halas, *Angew. Chem.* **46**, 9040 (2007).
- [35] S. Zhang, W. Ni, X. Kou, M. H. Yeung, L. Sun, J. Wang, and C. Yan, *Adv. Func. Mater.* **17**, 3258 (2007).
- [36] J. B. Liu, H. Dong, Y. M. Li, P. Zhan, M. W. Zhu, and Z. L. Wang, *Jpn. J. Appl. Phys.* **45**, L582 (2006).
- [37] S. K. Yang, W. P. Cai, L. C. Kong, and Y. Lei, *Adv. Func. Mater.* **20**, 2527 (2010).
- [38] R. Sainidou, N. Stefanou, and A. Modinos, *Phys. Rev. B* **69**, 064301 (2004).
- [39] V. Yannopapas and N. V. Vitanov, *Phys. Rev. B* **75**, 115124 (2007).
- [40] N. Stefanou, V. Yannopapas, and A. Modinos, *Comput. Phys. Commun.* **113**, 49 (1998); **132**, 189 (2000).
- [41] Z. Ficek and S. Swain, *Quantum Interference and Coherence: Theory and Experiments* (Springer, New York, 2005).
- [42] M. O. Scully, *Phys. Rev. Lett.* **67**, 1855 (1991).
- [43] M. Fleischhauer, C. H. Keitel, M. O. Scully, C. Su, B. T. Ulrich, and S.-Y. Zhu, *Phys. Rev. A* **46**, 1468 (1992).
- [44] A. Hatef, D. G. Schindel, and M. R. Singh, *Appl. Phys. Lett.* **99**, 181106 (2011).
- [45] Z. Zeng, E. Paspalakis, C. S. Garoufalidis, A. F. Terzis, and S. Baskoutas, *J. Appl. Phys.* **113**, 054303 (2013).